

# A modeling study of tidal energy extraction and the associated impact on tidal circulation in a multi-inlet bay system of Puget Sound

Taiping Wang\*, Zhaoqing Yang

Marine Sciences Laboratory, Pacific Northwest National Laboratory, 1100 Dexter Ave N, Ste 400, Seattle, WA, 98109, USA

## ARTICLE INFO

### Article history:

Received 5 October 2016

Received in revised form

15 February 2017

Accepted 16 March 2017

Available online xxx

### Keywords:

In-stream tidal energy

Modeling

Puget Sound

Agate Pass

Rich Passage

Tidal circulation

## ABSTRACT

Previous tidal energy studies in Puget Sound have focused on major deep channels such as Admiralty Inlet that have a larger power potential. This paper focuses on the possibility of extracting tidal energy from minor tidal channels of Puget Sound by using a hydrodynamic model to quantify the power potential and the associated impact on tidal circulation. The study site is a multi-inlet bay system connected by two narrow inlets, Agate Pass and Rich Passage, to the Main Basin of Puget Sound. A three-dimensional hydrodynamic model was applied to the study site and validated for tidal elevations and currents. We examined three energy extraction scenarios in which turbines were deployed in each of the two passages and concurrently in both. Extracted power rates and associated changes in tidal elevation, current, tidal flux, and residence time were examined. Maximum instantaneous power rates reached 250 kW, 1550 kW, and 1800 kW, respectively, for the three energy extraction scenarios. Model results suggest that with the level of energy extraction in the three energy extraction scenarios, the impact on tidal circulation is very small. It is worth investigating the feasibility of harnessing tidal energy from minor tidal channels of Puget Sound.

© 2017 Published by Elsevier Ltd.

## 1. Introduction

International Energy Outlook 2016 [1] projects worldwide energy demand will increase 48% from 549 quadrillion British thermal units (Btu) in 2012 to 815 quadrillion Btu in 2040. While fossil fuels will still account for 78% of energy use in 2040, renewable energy sources (e.g., solar power, hydropower, wind and tidal energy) remain the world's fastest-growing energy source over the projection period with an average increase rate of 2.6% per year between 2012 and 2040. Within this context and driven by the pressure in mitigating the threat of climate change, there has been a growing interest in harvesting energy from tidal currents with marine and hydro-kinetic (MHK) energy extraction devices because of the potential for tidal energy to be a viable source of clean and renewable energy. Compared to wind and solar energy, tidal energy is highly predictable in space and time. A rough estimate of total harvestable coastal tidal energy is around 1 TW worldwide [2]. With recent advancement in turbine design technology (e.g., Sea-Gen [3]), the economic and environmental costs of tidal energy

development are expected to be competitive with other energy sources. As a result, a series of tidal power demonstration projects have been carried out or planned to investigate the feasibility of commercial scale tidal energy development [3–5].

Meanwhile, a better understanding of the potential environmental and ecological impacts resulting from tidal energy development is needed [6]. Besides the "blade strike" threat to large marine organisms such as marine mammals, the interactions between tidal energy devices and the physical environment can lead to localized and even system-wide changes in flow fields and sediment transport [7,8]. For example, Neill et al. [8] demonstrated that a small amount of energy extracted from a tidal system can lead to a significant impact on the sediment dynamics, depending on tidal asymmetry at the point of extraction. Removal of a large amount of tidal energy can also result in substantial changes in tidal regime, potentially affecting communities living in intertidal zones [6,9,10]. In a modeling study conducted by Nash et al. [9] in Shannon Estuary, Ireland, the authors reported that the introduction of tidal stream turbines into the estuary can cause inter-tidal zones upstream of the turbine farm to be predominately inundated. Moreover, there is a practical need in determining the most suitable locations and turbine array configurations for energy extraction. To address the emerging needs associated with in-stream tidal energy

\* Corresponding author.

E-mail address: [taiping.wang@pnnl.gov](mailto:taiping.wang@pnnl.gov) (T. Wang).

development, numerical hydrodynamic models have been widely used to support tidal energy development [7–17]. These modeling studies covered a broad range of topics on tidal energy, including assessing the power potential and quantifying associated changes in near- and far-field velocity field, tidal regime, flushing rate and sediment transport. It was found, in general, that the effect of energy extraction on tidal regime and mass transport could be significant, depending on the amount and location of tidal energy extracted from the system. Therefore, it is highly recommended for in-stream tidal energy projects that a numerical modeling study should be conducted to evaluate potential project impacts on the physical environment and to provide critical information for making siting decisions.

The U.S. Pacific Northwest is considered a prime site for tidal energy development due to its unique geographic setting, which is characterized by a meso-macro tidal regime and numerous deep and constricted channels that feature strong tidal currents. For instance, harvesting tidal energy from Admiralty Inlet of Puget Sound, Washington to power residential homes has been a near decade-long joint effort by local, state and federal agencies and the power industry [18,19]. Besides Admiralty Inlet, other identified potential candidate sites in Puget Sound include constricted channels such as Tacoma Narrows, Deception Pass, Agate Pass and Rich Passage [18,20]. Previous modeling studies by Polagye et al. [21] and Yang et al. [22] also suggested that extracting a small fraction of available tidal energy from major channels like Admiralty Inlet and Tacoma Narrows is unlikely to have any significant system-wide impact.

In this paper, we investigated the possibility of extracting tidal energy from two narrow inlets of Puget Sound, namely Agate Pass and Rich Passage of West Puget Sound, as a continuation of our earlier study in Tacoma Narrows [22]. This study had dual objectives: to characterize the general tidal circulation pattern in a multi-inlet bay system that is connected to the main Puget Sound via Agate Pass and Rich Passage, and to quantify the potential impact on water circulation as a result of tidal energy extraction. This effort is the first modeling study in the Puget Sound region to investigate extracting tidal energy from relatively small-scale tidal channels. The results will provide useful information to stakeholders and the general public who are interested in harnessing tidal energy from Puget Sound waters.

## 2. Study site

Puget Sound is a complex, fjord-like estuarine system consisting of many interconnected marine waterways and basins that are connected to the East Pacific Ocean through the Strait of Juan de Fuca to the west and the Strait of Georgia to the north (Fig. 1). Located along the northwestern coast of the U.S. state of Washington, Puget Sound is the largest estuary in the country by volume and can be divided into four deep basins connected by shallower sills: Hood Canal, Whidbey Basin, South Sound, and the Main Basin, which is further subdivided into Admiralty Inlet and the Central Basin. With more than 4.5 million people living in the Puget Sound region and another 2.5 million expected by 2040, there has been a growing interest in harnessing tidal energy from the energetic waters of Puget Sound as a clean renewable energy source [18–20].

Previous tidal energy studies in Puget Sound focused primarily on major channels that have the highest power potential, such as Admiralty Inlet and Tacoma Narrows. While these major channels have the highest power potential, they also pose greater techno-economic challenges and environmental impacts, e.g., the high cost of installation and maintenance of energy extraction devices as well as the potential impacts on marine mammals and hydrodynamic circulation in the entire Puget Sound. In comparison, the tidal

energy extraction sites in this study, Agate Pass and Rich Passage (Fig. 1), are much smaller tidal channels that pose fewer techno-economic challenges. Water depth in Agate Pass is generally shallower than 10 m (NAVD 88) and the width varies from 300 to 500 m. Rich Passage is deeper and wider; its depth mostly varies from 20 to 30 m and it has a minimum width about 600 m. Together, Agate Pass and Rich Passage connect a multi-inlet bay complex (e.g., Port Orchard Passage, Liberty Bay, Dyes Inlet, and Sinclair Inlet) behind Bainbridge Island to the Central Basin of Puget Sound. This multi-inlet bay system forms the majority of West Puget Sound, a geographic action area defined in the Puget Sound Action Agenda [23]. As a tidally dominated system with an average freshwater to tidal prism ratio of 0.3%, tides propagate into the multi-inlet bay system through two narrow inlets and produce currents greater than 2 m/s that are sufficient to drive tidal turbines. On the other hand, extracting energy from Agate Pass and Rich Passage may reduce tidal flows through these passages and potentially affect tidal circulation in the system. Therefore, the model domain covered a much broader area with a focus on the multi-inlet bay system.

## 3. Methodology

### 3.1. Hydrodynamic model with an embedded MHK module

The hydrodynamic model used for this study is the unstructured-grid, finite-volume, community ocean model (FVCOM) [24–26]. As a general purpose three-dimensional (3-D) coastal ocean model, FVCOM simulates water surface elevation, velocity, salinity, temperature, sediment, and other scalar constituents in an integral form by computing fluxes between non-overlapping horizontal triangular control volumes. By using unstructured triangular cells in the horizontal plane and a sigma-stretched coordinate system in the vertical direction, the model is especially suitable for representing the complex horizontal geometry and bottom topography of estuaries like Puget Sound [27]. It also allows for greater flexibility and computational efficiency in simulating tidal energy extraction that often requires fine grid resolution in the region of a tidal turbine farm embedded within a large model domain [17,22].

To simulate the effect of tidal energy extraction, a MHK module has been implemented in the FVCOM model using the momentum sink approach [14]. The MHK module was validated against both the analytical solution [14] and laboratory flume experiment [28], and was subsequently applied to study tidal energy extraction in Tacoma Narrows [22]. Specifically, the momentum governing equations for Reynolds-averaged turbulent flows with momentum sink terms due to energy extraction have the following general form [14]:

$$\frac{\partial u}{\partial t} + u \frac{\partial u}{\partial x} + v \frac{\partial u}{\partial y} + w \frac{\partial u}{\partial z} - fv = -\frac{1}{\rho_0} \frac{\partial p}{\partial x} + \frac{\partial}{\partial z} \left( K_m \frac{\partial u}{\partial z} \right) + F_x - F_x^M \quad (1)$$

$$\frac{\partial v}{\partial t} + u \frac{\partial v}{\partial x} + v \frac{\partial v}{\partial y} + w \frac{\partial v}{\partial z} + fu = -\frac{1}{\rho_0} \frac{\partial p}{\partial y} + \frac{\partial}{\partial z} \left( K_m \frac{\partial v}{\partial z} \right) + F_y - F_y^M \quad (2)$$

where  $(x, y, z)$  are the east, north, and vertical axes in the Cartesian coordinates;  $(u, v, w)$  are the three velocity components in the  $x$ ,  $y$ , and  $z$  directions;  $(F_x, F_y)$  are the horizontal momentum diffusivity terms in the  $x$  and  $y$  directions;  $K_m$  is the vertical eddy viscosity coefficient;  $\rho$  is water density;  $p$  is pressure; and  $f$  is the Coriolis parameter.  $\overline{F^M} = (F_x^M, F_y^M)$  are the turbine-induced momentum sink

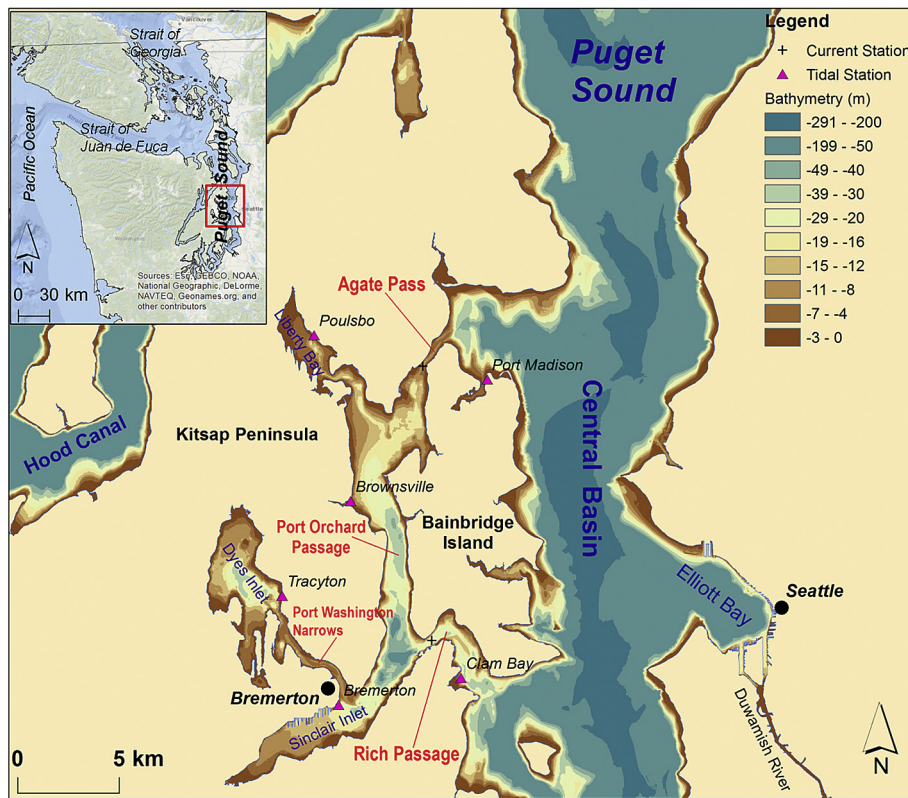


**Fig. 1.** Study area – the multi-inlet bay system connected by Agate Pass and Rich Passage to Central Basin of Puget Sound, Washington, USA. The six tidal stations and two current stations are indicated with triangle and cross symbols, respectively. Bathymetry is referenced to NAVD 88 vertical datum.

terms that are defined as follows:

$$\overline{F^M} = \frac{1}{2} \frac{C_T A}{V_c} |\overline{u}| \overline{u} \quad (3)$$

where  $V_c$  is the control volume,  $C_T$  is the turbine thrust coefficient,  $A$  is the flow-facing area swept by the turbines, and  $\overline{u}$  is the velocity vector at hub height. The total extracted tidal power at any given time can be calculated based on the following formula:

$$P_{\text{total}} = \sum_{i=1}^M \left( N \times \frac{1}{2} \rho C_T A |\overline{u}|^3 \right)_i \quad (4)$$

where  $N$  is the number of turbines in each grid element (or momentum control volume) and  $M$  is the total number of elements containing turbines.

### 3.2. Model configuration

Although the focus of this study was mainly on a sub-basin in West Puget Sound, we chose to model it together with the entire Puget Sound by leveraging from the previous modeling work, such that any potential far-field impact resulting from energy extraction in Agate Pass and Rich Passage could be examined. The model grid used for this study was adopted from the one used by Yang and Khangaonkar [27] and Yang and Wang [29], which covers the entire Puget Sound, Strait of Juan de Fuca, and Strait of Georgia, and was further refined for the study site (Fig. 2). The model grid size varies from approximately 80 m at Agate Pass and Rich Passage to more than 2000 m at the two open boundaries, which end at the entrance of Strait of Juan de Fuca along the Pacific Ocean and northern end of Strait of Georgia, respectively.

Model configuration generally follows that reported in earlier studies [27,29]. At the open boundaries, predicted harmonic tides by XTide program [30] at tidal stations Neah Bay, Washington and Campbell River, British Columbia were specified at 15-min intervals. The horizontal mixing scheme uses the Smagorinsky parameterization [31], and the vertical mixing is calculated using the Mellor–Yamada level 2.5 turbulent closure [32]. The bottom friction is described by the quadratic law and the drag coefficient is determined by the logarithmic bottom layer as a function of prescribed bottom roughness. A minimum bottom drag coefficient of 0.0025 and a uniform bottom roughness of 0.001 m were used. In the vertical direction, three uniform sigma layers were specified to capture the vertical structure of tidal flows.

Although the West Puget Sound was included in earlier modeling efforts [27,29], neither tidal calibration nor the general circulation pattern has been examined. The only hydrodynamic modeling study of the West Puget Sound is the modeling project conducted by Wang et al. [33] in the early 2000s. However, their model domain only covered the southern part of the Agate Pass – Rich Passage complex, i.e., the southern half of Port Orchard Passage, Rich Passage, and Sinclair and Dyes Inlets. In this study, we conducted a year-long simulation for 2006 and compared model predicted tidal elevations against XTide predictions at six stations throughout the study area (Fig. 1). The year-long simulation established a robust baseline condition for us to characterize the general circulation pattern in the study site, which can be further compared with that under different tidal energy extraction scenarios to examine any potential changes in tidal circulation. River inflows as well as density-induced and wind-driven circulation were not included because this study mainly focused on the barotropic tidal circulation. Lastly, all model runs were conducted with double precision to minimize the

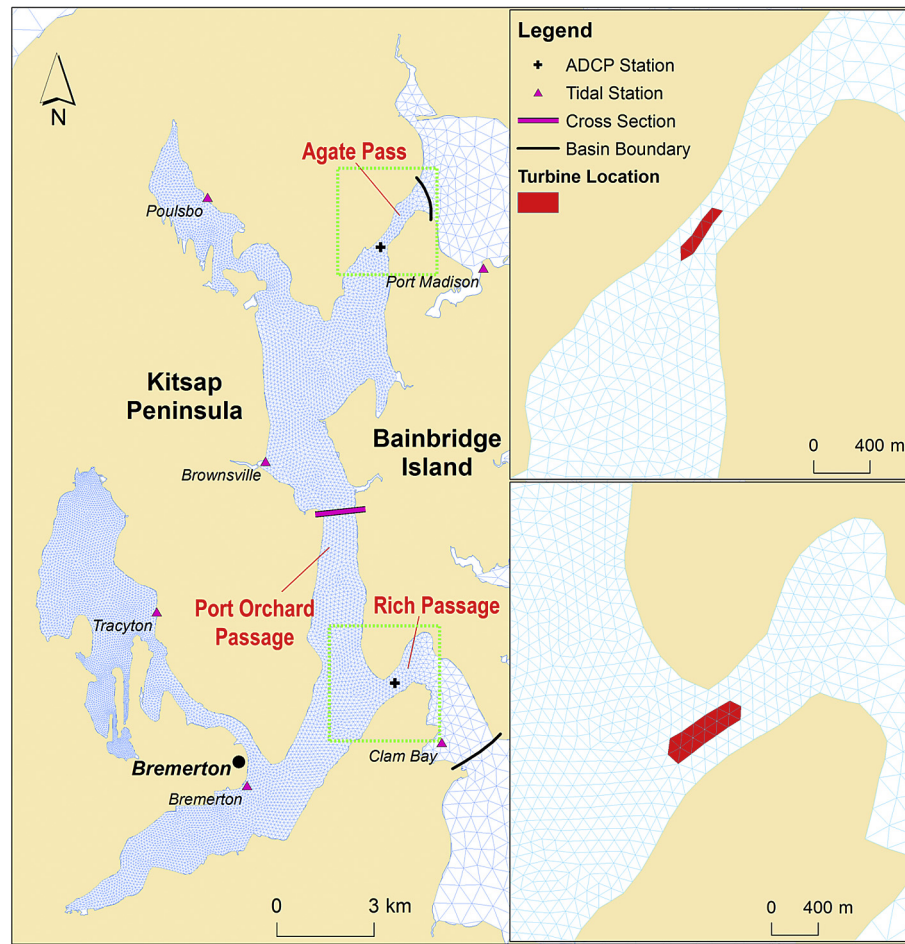


**Fig. 2.** Unstructured model grid for the study area with zoom-in views in Agate Pass and Rich Passage showing grid elements with tidal turbines deployed. The interconnected multi-inlet bay complex delimited by the basin boundary lines outside Agate Pass and Rich Passage is the focus area of this study. The cross-section line in Port Orchard Passage shows the cross-section where the tidal flux was examined and presented in Fig. 6 and 10.

truncation error that could potentially affect the accuracy of model results.

### 3.3. Tidal energy extraction scenarios

The locations of the tidal turbine farm were determined based on model predicted maximum depth-averaged tidal currents greater than 2 m/s and water depths deeper than 8 m (NAV88). The depth criterion of 8 m was selected mainly because of the shallowness of Agate Pass. While a larger depth criterion will allow for better navigation safety, it will further reduce the area suitable for turbine deployment. The grid elements identified as suitable energy extraction sites are shown in Fig. 2. The tidal turbines were assumed to be bottom-mounted axial turbines that have a diameter of 3 m and a hub height of 2.5 m. The turbine thrust coefficient was specified as 0.8 for all model runs based on typical literature values [34,35]. In this study, we only examined one example turbine array configuration by specifying the turbine density as five turbines per grid element. Because the surface area of the grid elements in the channels is greater than 5000 m<sup>2</sup> and much larger than the turbine dimension, numerically there is no difference in the actual turbine array layout in each grid element. At both channels, the blockage ratio of the cross-sectional area is smaller than 1%. For simplicity, energy dissipated by the turbine supporting structures was neglected. Three energy extraction scenarios were examined, i.e., energy was only extracted from one of the channels and

concurrently from both. Hereafter, these scenarios were defined by order as Agate Pass only, Rich Passage only, and both passages. Together with the baseline condition in which no energy extraction was simulated, a total of four separate model runs were conducted.

### 3.4. Residence time calculation

In addition to quantifying the changes in tidal elevation, current, and volume flux that resulted from tidal energy extraction, the residence time was calculated for the baseline condition and three energy extraction scenarios to examine the cumulative effect of energy extraction on tidal circulation. The same modeling approach used for determining the flushing capability of Bellingham Bay in northern Puget Sound [36] was adopted for this study. The averaged residence time of all the water parcels inside the area of interest can be calculated based on the remnant function defined by Takeoka [37]:

$$RT = \int_0^{\infty} \frac{R(t)}{R_0} dt \quad (5)$$

where RT is the basin-wide averaged residence time. By assuming the initial amount of a neutrally buoyant conservative tracer (dye) in a waterbody at  $t = 0$  as  $R_0$  and the amount of tracer that still remains in the system at time  $t$  as  $R(t)$  (i.e. the amount of tracer

whose  $RT$  is larger than  $t$ ),  $R(t)/R_0$  is called the remnant function [37]. Equation (5) can be solved by integrating model-calculated tracer concentration/mass time series to give the averaged residence time for the entire area of interest.

## 4. Results and discussion

### 4.1. Model validation and general circulation pattern

Because water level observations are very limited for the study site, we chose to validate the hydrodynamic model using XTide predictions [30], which are essentially the same astronomical tidal predictions provided by the National Oceanic and Atmospheric Administration (NOAA). Fig. 3 shows the time series comparisons between FVCOM simulations and XTide predictions during a two-week spring-neap cycle in year 2006, the same year in the previous Puget Sound hydrodynamic modeling study [27]. Two representative error statistical parameters, the coefficient of determination ( $R^2$ ) and the root-mean-square error (RMSE), were calculated and included with the plot. As indicated by the error statistical parameters, the model predicted tidal elevations match XTide predictions very well at all stations. The spring-neap tidal cycle and the diurnal inequality were successfully reproduced by the model. In general, tides inside the multi-inlet bay system are mixed semi-diurnal and closely resemble the two outside stations (Port Madison and Clam Bay), except for the most upstream station, Tracyton in Dyes Inlet, at which there is noticeable phase lag and amplitude amplification.

In summer 2015, NOAA conducted a current survey using the Acoustic Doppler Current Profiler (ADCP) at various locations of Puget Sound, including Agate Pass and Rich Passage (see Figs. 1 and

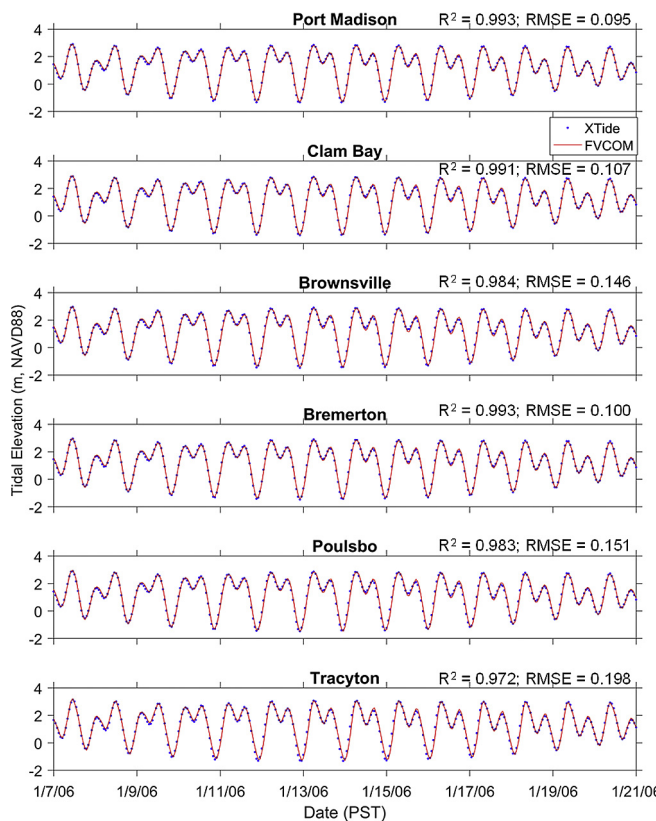


Fig. 3. Tidal calibration at six stations throughout the study site (see Fig. 1 and 2 for location information). The unit for RMSE values is meter(s).

2 for ADCP locations). The survey data have been uploaded to NOAA's C-MIST website (<https://cmist.noaa.gov/cmist/>) and the survey period normally lasted for about a month at each station. To further validate the hydrodynamic model for tidal currents that are critical for tidal energy projects, we set up the model for August 2015 using the same model configuration described above. The ADCP data were collected at 6-min intervals and for eight vertical bins through the water column. For model-data comparison, we first calculated the depth-averaged East-West (U) and North-South (V) velocity components for both model predictions and ADCP measurements and then projected them onto the along-channel principal axis. The time series comparisons are shown in Fig. 4. Similar to tidal elevation comparisons, the current predictions compared very well to data ( $R^2 > 0.97$  and  $RMSE < 0.15$  m/s) for both passages. In addition, current asymmetry can be seen at both locations – Agate Pass is flood dominated, while Rich Passage shows slight ebb dominancy.

Fig. 5 provides snapshots of model predicted depth-averaged tidal currents at flood and ebb in November 2006. In spite of current magnitude reaches 2 m/s at places in Agate Pass and Rich Passage, the currents are relatively weak for the rest of the system. For instance, in Port Orchard Passage, the strait behind Bainbridge Island connecting Agate Pass and Rich Passage, the current magnitude is mostly smaller than 0.2 m/s, and tidal flows are dominated by Rich Passage (Fig. 5c and d) during both flood and ebb tides. Fig. 6 shows the tidal flux through the cross-section (see Fig. 2 for location) located in the middle of Port Orchard Passage that connects Agate Pass and Rich Passage. The peak tidal flux at both flood and ebb exceeds 4000 m<sup>3</sup>/s. Despite some small fluctuations in the tidal flux curve, the result does suggest that at most times, positive tidal flux values (flows from Rich Passage to Agate Pass) correspond to the rising tides, and vice versa. This is consistent with the flow field observed in Fig. 5.

### 4.2. Tidal energy extraction in Agate Pass and Rich Passage

Fig. 7 shows the instantaneous extracted tidal power time series under three different energy extraction conditions. The extracted

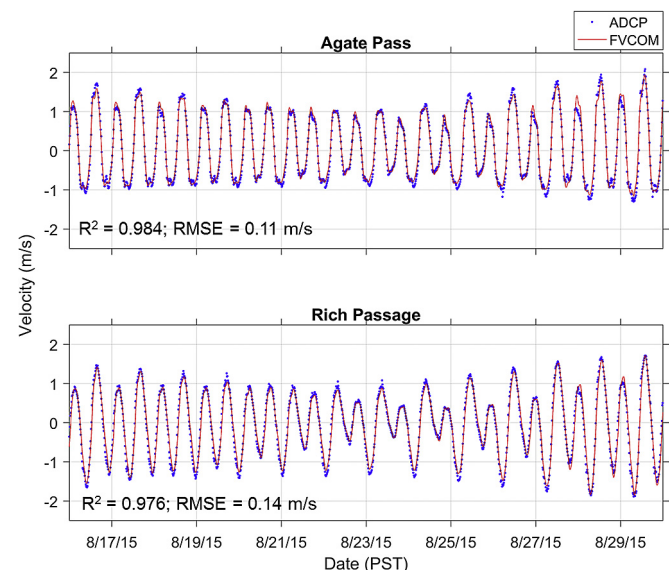
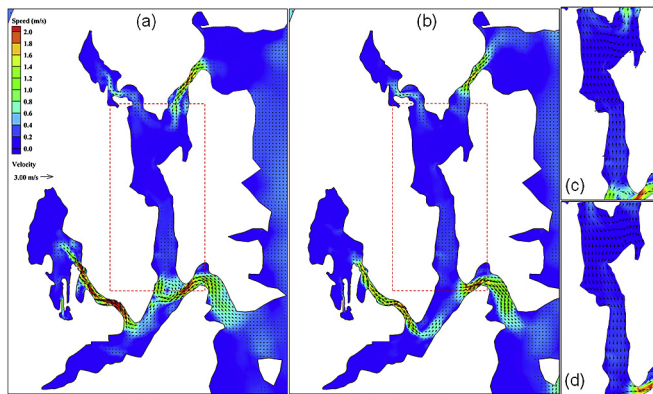
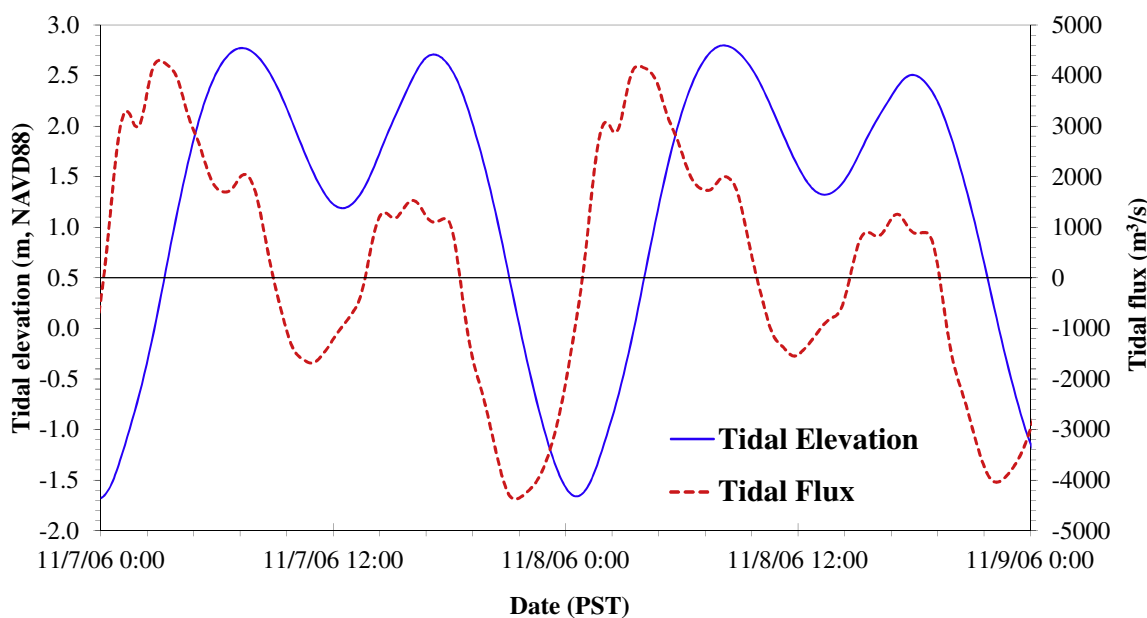


Fig. 4. Velocity comparisons between model predictions and ADCP measurements at Agate Pass and Rich Passage (see Fig. 2 for ADCP locations). Velocities have been projected to the principal axis along the channels with positive values during the flooding tide (flowing into the multi-inlet bay system).



**Fig. 5.** Snapshots of depth-averaged tidal velocity at flood (a,c, 11/7/2006 3:30 a.m.) and ebb (b,d, 11/7/2006 9:30 p.m.). Velocity vectors in (c) and (d) are exaggerated and not to scale.

power was calculated using Equation (4). The power time series exhibit strong temporal variations over spring and neap tidal cycles due to the complexity of tidal currents in both passages. The extractable power during spring tides is nearly an order of magnitude greater than during neap tides; this is expected because the extracted power is proportional to the cube of tidal velocity (Equation (4)). The maximum instantaneous power rate calculated with Equation (4) reaches approximately 250 kW, 1550 kW, and 1800 kW respectively under three energy extraction scenarios. The extracted power rate from Rich Passage is considerably larger than that from Agate Pass, mainly because the former allowed for more turbines (110 vs. 35). For the scenario with turbines deployed in both passages, the instantaneous extracted power is roughly equal to the sum of the other two scenarios in which turbines were only deployed in one of the passages. By averaging the instantaneous power time series for the entire year of 2006, the annual mean power rates for three energy extraction scenarios are 42.3 kW,



**Fig. 6.** Tidal flux through the cross-section (see Fig. 2 for location) in the middle of Port Orchard Passage that connects Agate Pass and Rich Passage vs. tidal elevations at the central location of the cross-section. Positive flux values indicate flows from Rich Passage to Agate Pass (northward).

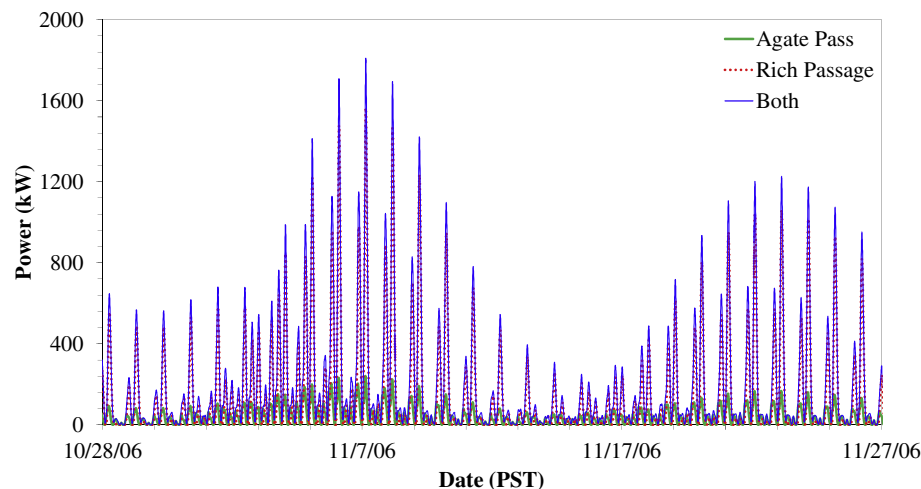


**Fig. 7.** Instantaneous extracted tidal power under three extraction scenarios over a 30-day simulation period.

150.1 kW, and 194.0 kW, respectively. The mean power extracted concurrently from both passages (194.0 kW) is slightly higher than the linear summation (192.4 kW) of the two scenarios in which power was extracted separately from one of the passages. It should be noted that this power estimation is a theoretical value calculated by the hydrodynamic model. Considering that most MHK devices require a cut-in speed to produce power, the actual power production rate should be smaller.

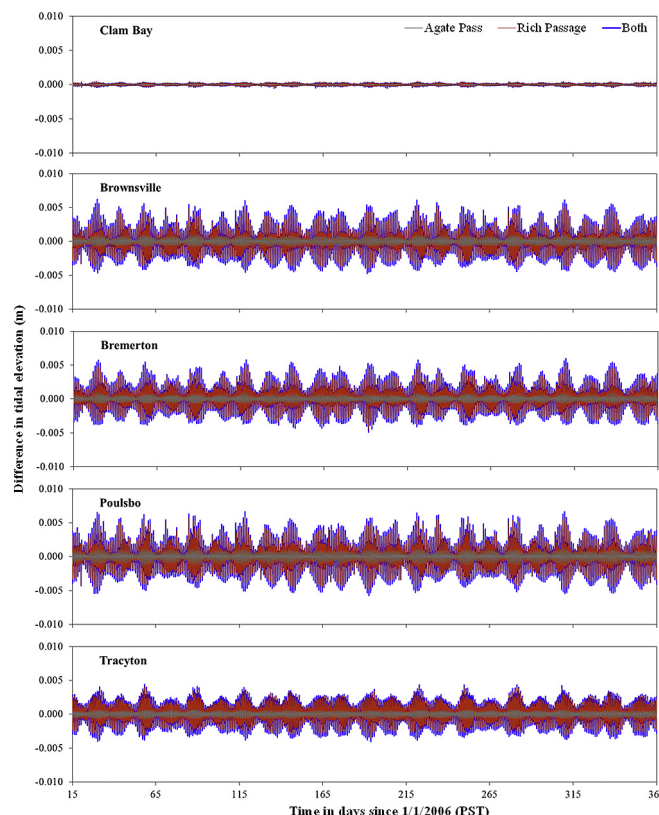


**Fig. 8.** The impact of energy extraction on tidal elevations under three energy extraction scenarios. The results shown are calculated elevation differences between energy extraction scenarios and the baseline condition at five tidal stations indicated in Fig. 1 and 2.

#### 4.3. Impacts of energy extraction on tidal circulation

##### 4.3.1. Impact on tidal range

One major concern related to extracting tidal energy from an entrance channel is its potential impact on natural tidal regimes. The most obvious change is the decrease in tidal range in the basin behind the channel. We examined the changes in tidal elevation under all three energy extraction scenarios and calculated the differences from the baseline condition. The results are presented in Figs. 8 and 9. Fig. 8 shows the elevation differences at five tidal stations during the one year simulation period. The impact of energy extraction is mainly on stations inside the multi-inlet bay system behind the two passages. The elevation difference appears to correlate with the amount of energy extracted from the system, and the maximum is smaller than 0.8 cm at all four stations inside the system. Considering that the tidal range varies from 1 to 4 m, the change in tidal elevation is very small. At Clam Bay station outside Rich Passage, the elevation change is even smaller compared to inside stations and generally negligible. Fig. 9 provides a closer look at Brownsville station in Port Orchard Passage over a two-week spring-neap tidal cycle. Because the momentum extraction rate by turbines is proportional to velocity square (Equation (3)), the elevation difference varies with the range and phase of tides with maximum values occurring during spring tides and near peak ebb and flood tidal stages. This is consistent with the findings by Yang et al. [22].

##### 4.3.2. Impact on tidal flux

The change in tidal elevation affects both tidal prism and tidal flux in and out of the system through the entrance. The decrease in tidal flux will reduce the flushing capability of a tidal system, which may lead to water quality issues such as eutrophication [38]. Fig. 10 shows the differences in total tidal flux between three energy extraction scenarios and the baseline condition. Compared to total tidal flux under the baseline condition that varies between  $\pm 30,000 \text{ m}^3/\text{s}$ , the difference in the change of tidal flux between energy extraction scenarios and the baseline condition is much smaller, e.g., generally on the order of  $\pm 100 \text{ m}^3/\text{s}$ , or about 0.3% of the total tidal flux. Similar to the change in tidal elevation presented in Figs. 8 and 9, the change in tidal flux positively correlates with total tidal flux in and out of the system. The tidal flux time series in Fig. 10 also suggests that this multi-inlet bay system is slightly

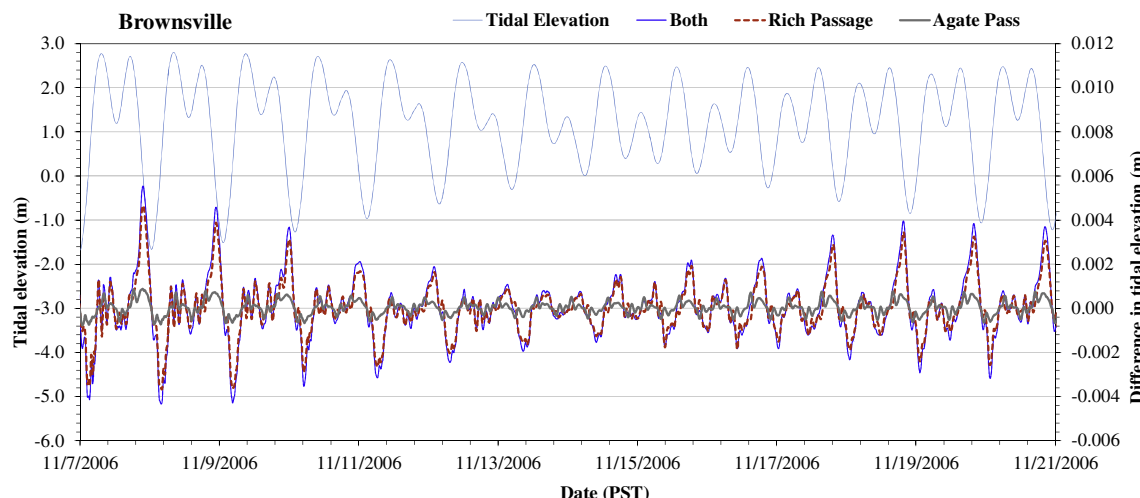


**Fig. 9.** The impact of energy extraction on tidal elevations at Brownsville station under three energy extraction scenarios. The results shown here are elevation differences between energy extraction scenarios and the baseline condition. The tidal elevation time series was extracted from the same station for reference.

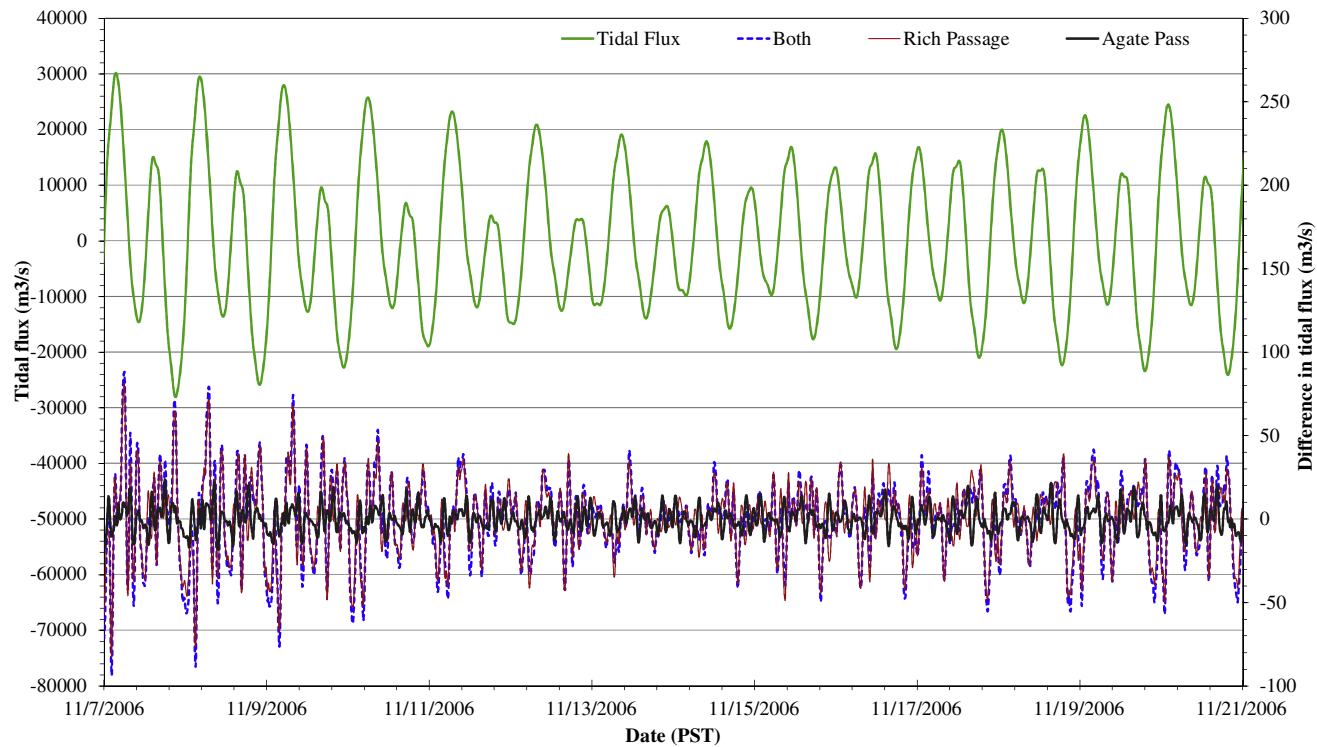


**Fig. 10.** The differences in total tidal flux in and out of the multi-inlet bay system through both Agate Pass and Rich Passage between three energy extraction scenarios and the baseline condition vs. total tidal flux in the baseline condition (positive values denote tidal flows into the system).

flood-dominated; the magnitude of incoming tidal flows is slightly larger than that of ebbing flows.

In previous sections, we discussed that tidal circulation in the system is dominated by flows from Rich Passage (Figs. 5 and 6). With energy being extracted from one or both of the passages, the

natural circulation pattern could be changed. This potential change was examined by comparing the change in tidal flux through the cross-section in the middle of Port Orchard Passage (see Fig. 2 for the cross-section location). Fig. 11 shows the change in tidal flux between three energy extraction scenarios and the baseline

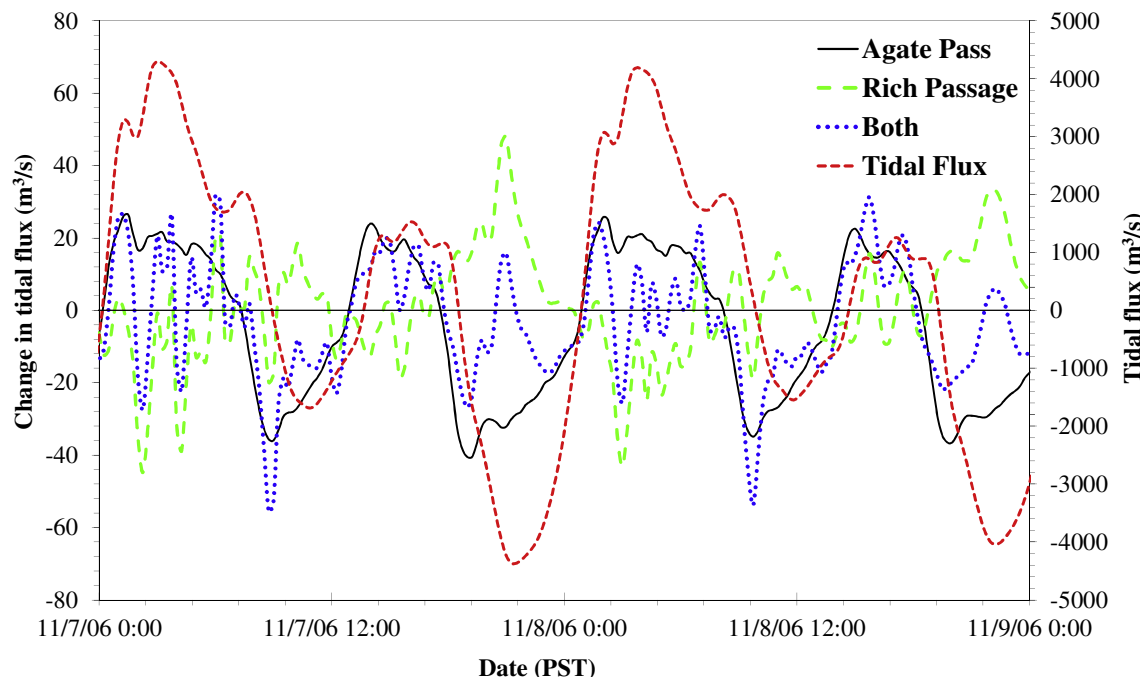


**Fig. 11.** The change in tidal flux through the cross-section (see Fig. 2 for location) in the middle of Port Orchard Passage that connects Agate Pass and Rich Passage between the three energy extraction scenarios and the baseline condition. The tidal flux curve (red dash line plotted on the right Y-axis) is the same at that in Fig. 6, and positive flux values indicate flows from Rich Passage to Agate Pass (northward). (For interpretation of the references to colour in this figure legend, the reader is referred to the web version of this article.)

condition. It seems that the change in tidal flux due to energy extraction in Agate Pass closely follows the total tidal flux in the baseline condition despite a phase lag. This suggests that extracting tidal energy in Agate Pass reduces tidal flow through it. As a result, more water flows north (from Rich Passage) during flood tide and vice versa. Although the magnitude is relatively small (on the order of  $\pm 40$  m<sup>3</sup>/s, or ~1% of the total tidal flux through the cross-section during the baseline condition during the spring tide), it indicates the impact of energy extraction on tidal flow through Agate Pass is evident. Compared to Agate Pass, the change in tidal flux as a result of energy extraction in Rich Passage appears to be more complex. However, the general trend is negatively correlated with the total tidal flux in the baseline condition. Interestingly, although more energy is extracted from Rich Passage, the effect on the change in tidal flux is comparable to that of Agate Pass. This is because Rich Passage is much deeper and wider than Agate Pass and allows more flow to bypass the turbines. Lastly, the change in tidal flux for the last scenario, in which energy is extracted from both passages, seems to be the linear combination of the first two scenarios.

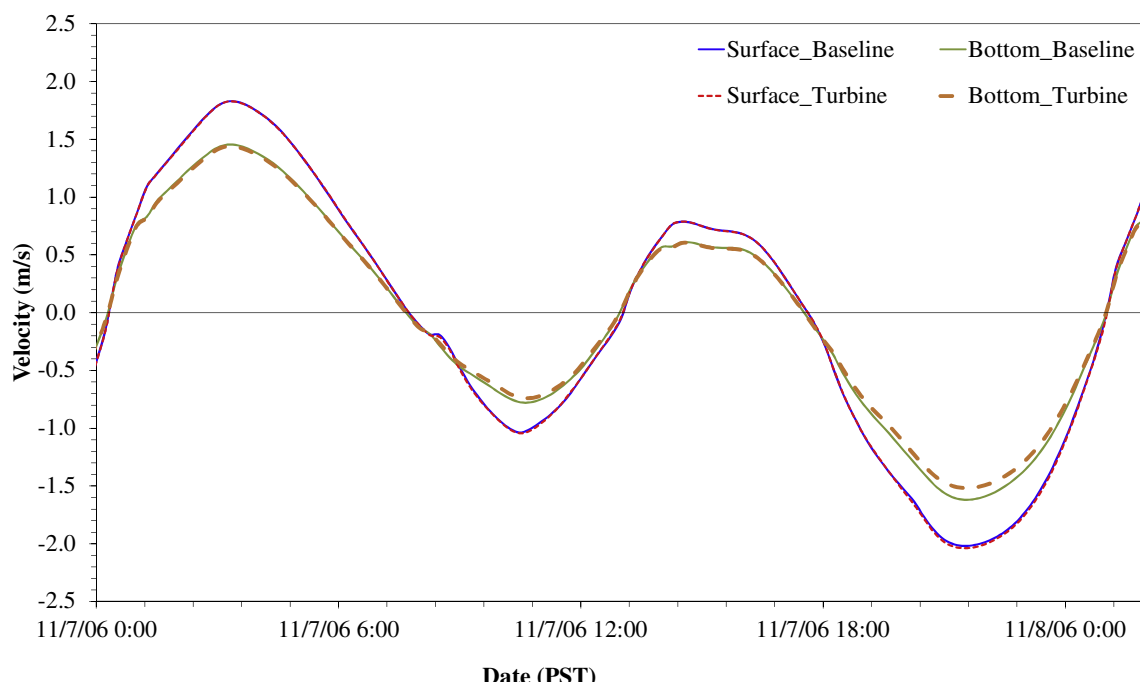
#### 4.3.3. Impact on tidal velocity

Fig. 12 shows the impact of energy extraction on velocity profiles at one grid element in Rich Passage with energy extraction. The result is for two tidal cycles during a spring tide. For the bottom layer where tidal turbines are deployed, an overall decrease in the current magnitude due to energy extraction is obvious. The maximum difference is on the order of 0.1 m/s at the peak ebb. In comparison, there is a slight increase at the surface layer, as a result of the “flow bypass” effect observed in similar modeling studies [14,17]. We further examined system-wide changes in tidal velocity. Instead of checking velocity distribution at a specific time, we chose to quantify the change in median values of current speed for the full-year simulation. As one can see from Fig. 13, median current magnitude is generally smaller than 0.8 m/s for the study site, and high values primarily occur in the narrow channels. The impact of tidal energy extraction on tidal currents is also limited to areas

surrounding the locations where energy is extracted (Fig. 13b–d). The percentage change in current speed varies from –18% to 14% inside the model domain with similar spatial distribution patterns (results not shown). The results also suggest that extracting energy from one of the two entrance channels alone will slightly increase current speed (<3 mm/s) at the other channel (Fig. 13b and c). Extracting energy concurrently from both channels appears to have a broader impact, which, appears to be the combination of that caused by individual energy extraction conditions. Similar to the “flow bypass” effect observed in Fig. 12, extracting energy from the middle of the channel also increases current speed on the side of the channel (Fig. 13b–d) and may increase the potential for bank erosion. Despite the overall magnitude of change in median current speed is only on the order of a few centimeters per second, the spatial pattern is relatively complicated. Interestingly, this pattern appears to indicate that the change in current speed alternates between positive (increase) and negative (decrease) values surrounding the turbine locations.

#### 4.3.4. Impact on residence time

Transport timescales such as residence time are a useful quantitative indicator to illustrate the role contributed by physical circulation to biogeochemical processes of a waterbody [39]. The changes in residence time were calculated for the entire multi-inlet bay system using Equation (5) by releasing dye instantaneously to the entire multi-inlet bay system, i.e., the whole basin was filled by neutrally-buoyant dye with a uniform concentration of 1 mg/L during model simulations. Residence time was then calculated for each scenario using Equation (5) based on the remaining dye mass inside the multi-inlet bay system. The model-calculated system-wide residence time values at the end of one year simulation period are 33.84, 33.84, 33.98, and 33.99 days, respectively, for the baseline and three energy extraction conditions defined earlier. Obviously, the differences are very small among all the scenarios. Compared to the baseline condition, system-wide residence time only increases 0.15 day or 0.44% for the scenario with most energy



**Fig. 12.** Velocity comparisons between the baseline condition and the scenario in which tidal energy was extracted from Rich Passage. The location was randomly picked from the grid elements in Rich Passage where tidal turbines were deployed.

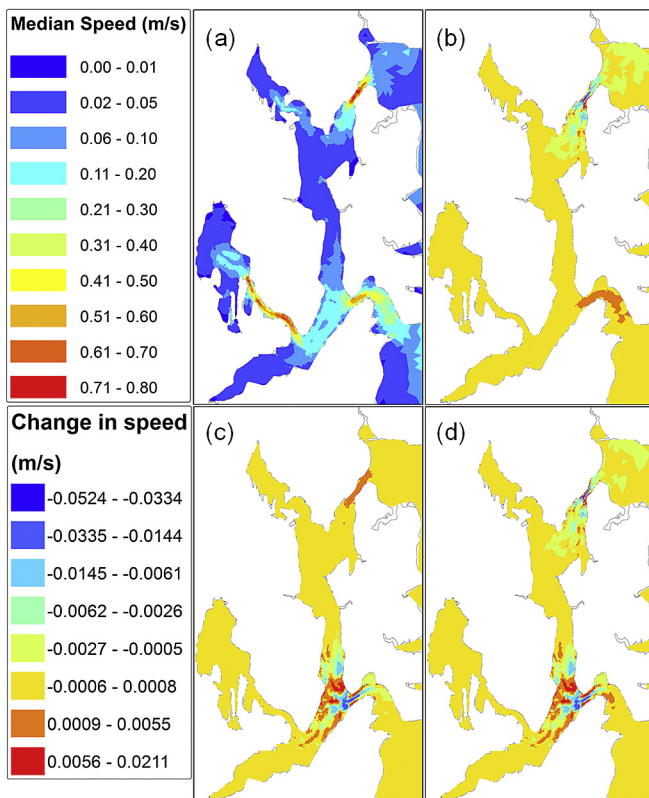


**Fig. 13.** Median current speed distribution at the bottom layer for the baseline condition during the full-year simulation (a); and changes in median current speed under three energy extraction scenarios compared to the baseline condition (b–d).

extraction. Therefore, from a system-wide perspective, it is reasonable to conclude that the system is unlikely to experience any obvious changes in its ecological responses such as a substantial increase in fecal coliform bacteria concentration for the level of energy extracted in this study. Fig. 14 shows the difference in dye concentration (which was initialized with a concentration of 1.0 inside the entire multi-inlet bay system) between the full

energy extraction scenario and the baseline condition at Days 30 and 200, respectively, following the dye release. The differences are minimal for most areas except for Port Orchard Passage where tidal circulation is dominated by both entrances. The relative change in dye concentration at one location of Port Orchard Passage exceeds 10% after a 200-day simulation, suggesting that certain areas of Port Orchard Passage are more sensitive to energy extraction. However, because major water quality issues (e.g., fecal coliform bacteria and toxic contamination) primarily occur in Dyes and Sinclair Inlets where the change in dye concentration is minimal, it is expected that these existing water quality issues should not be affected by the proposed level of energy extraction in this study.

## 5. Summary

In the study reported here, we investigated the possibility of extracting tidal energy from two tidal energy candidate sites (Agate Pass and Rich Passage) identified by previous studies in Puget Sound [18,20]. By using the 3-D hydrodynamic model FVCOM with an embedded MHK module, we quantified the power production rates and associated impacts on tidal circulation under three energy extraction scenarios. The results suggest that with the example turbine array configuration proposed in this study, the resulting effects on tidal circulation are very small, as reflected by the quantitative changes in major physical variables including tidal range, current, tidal flux, and residence time.

Unlike major tidal channels, such as Admiralty Inlet, that have a larger potential for power extraction and often pose greater technical challenges, Agate Pass and Rich Passage are relatively small tidal inlets that provide easier access for tidal turbine deployment and maintenance. Although the extractable power rate is smaller compared to major tidal channels, the small tidal channels still provide an alternative, renewable energy resource that can become especially useful in the event of emergency conditions (e.g., natural disasters) when conventional energy supplies are disrupted. Moreover, we only examined one example turbine configuration (e.g., dimension and layout); it is expected that higher tidal power rates can be produced by increasing turbine density and size especially in Rich Passage where water depth is deeper. Based on the findings of this study, we can reasonably predict that extracting more power from the system with a practically feasible turbine configuration should not cause system-wide environmental concerns. Considering the physical constraints and relatively low power potential of Agate Pass, extracting power from Rich Passage seems to be a more feasible option. Port Washington Narrows could be another candidate site due to its higher power density and proximity to urban infrastructure.

Lastly, this study is the first 3-D hydrodynamic modeling study focusing on the entire multi-inlet bay system that is connected by Agate Pass and Rich Passage to the Central Basin of Puget Sound. The model was validated for tides and further used to characterize the general circulation pattern driven by tides. The estimated residence time can provide useful information for studying contaminant transport in system [40]. It should be mentioned that the actual circulation and residence time may vary from the model results presented in this study because they are affected by the combination of tides, meteorological forcing, and river input. In the future, the model can be further refined by incorporating more physical and biogeochemical processes to support a more thorough assessment of tidal energy extraction.

## Acknowledgments

This study was conducted by leveraging previous modeling tools that were developed with support from the Water Power Program

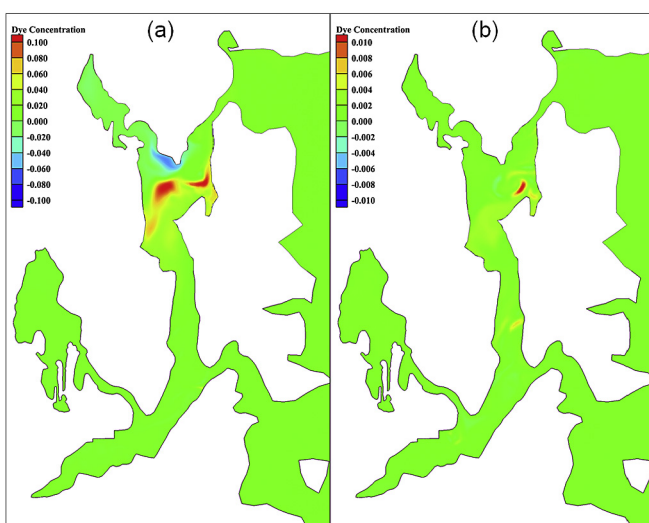


**Fig. 14.** Difference in dye concentration field (mg/L) between the energy extraction scenario (energy extracted from both tidal channels) and the baseline condition on Day 30 (a) and Day 200 (b), respectively.

within the Office of Energy Efficiency and Renewable Energy, U.S. Department of Energy under contract DE-AC05-76RL01830 to Pacific Northwest National Laboratory. We also thank PNNL Institutional Computing (PIC) Program for providing computational resource to this study.

## References

- [1] EIA International Energy Outlook, 2016. [http://www.eia.gov/forecasts/ieo/exec\\_summ.cfm](http://www.eia.gov/forecasts/ieo/exec_summ.cfm).
- [2] Schweitzer, Sophia. "Will tidal and wave energy ever live up to their potential?". *Yale Environ. 360*. (Accessed 10 September 2016).
- [3] C.A. Douglas, G.P. Harrison, J.P. Chick, Life cycle assessment of the seagen marine current turbine, *Proc. Inst. Mech. Eng. Part M: J. Eng. Maritime Environ. Prof. Eng. Publ.* 222 (2008) 1–12, <http://dx.doi.org/10.1243/14750902JEME94>.
- [4] <http://www.racerocks.ca/tidal-current-energy-demonstration-project-renewable-energy-for-race-rocks/> (Accessed 10 September 2016).
- [5] <http://www.verdantpower.com/rite-project.html> (Accessed 10 September 2016).
- [6] G. Boehlert, A. Gill, Environmental and ecological effects of ocean renewable energy development: a current synthesis, *Oceanography* 23 (2010) 68–81.
- [7] D. Hasegawa, J. Sheng, D. Greenberg, K. Thompson, Far-field effects of tidal energy extraction in the Minas Passage on tidal circulation in the Bay of Fundy and Gulf of Maine using a nested-grid coastal circulation model, *Ocean. Dyn.* 61 (2011) 1845–1868.
- [8] S.P. Neill, E.J. Litt, S.J. Couch, A.G. Davies, The impact of tidal stream turbines on large-scale sediment dynamics, *Renew. Energy* 34 (2009) 2803–2812.
- [9] S. Nash, N. O'Brien, A. Obert, M. Hartnett, Modeling the far field hydro-environmental impacts of tidal farms – a focus on tidal regime, inter-tidal zones and flushing, *Comput. Geosci.* 71 (2014) 20–27.
- [10] J.D. Goss-Custard, R.M. Warwick, R. Kirby, S. McGroarty, R.T. Clarke, B. Pearson, W.E. Rispi, S.E.A. Le, V. Dit Durell, R.J. Rose, Towards predicting wading bird densities from predicted prey densities in a post-barrage Severn estuary, *J. Appl. Ecol.* 28 (1991) 1004–1026.
- [11] G. Sutherland, M. Foreman, C. Garrett, Tidal current energy assessment for johnstone strait, vancouver Island, *Proc. Inst. Mech. Eng. Part A J. Power Energy* 221 (2007) 147–157.
- [12] R. Karsten, J. McMillan, M. Lickley, R. Haynes, Assessment of tidal current energy in the minas passage, bay of fundy, *Proc. Inst. Mech. Eng. Part A J. Power Energy* 222 (2008) 493–507.
- [13] Z. Defne, K.A. Haas, H.M. Fritz, Numerical modeling of tidal currents and the effects of power extraction on estuarine hydrodynamics along the Georgia coast, USA, *Renew. Energy* 36 (2011) 3461–3471.
- [14] Z. Yang, T. Wang, A.E. Copping, Modeling tidal stream energy extraction and its effects on transport processes in a tidal channel and bay system using a three-dimensional coastal ocean model, *Renew. Energy* 50 (2013) 605–613.
- [15] S.P. Neill, M.R. Hashemi, M.J. Lewis, The role of tidal asymmetry in characterizing the tidal energy resource of Orkney, *Renew. Energy* 68 (2014) 337–350.
- [16] J. Thiébot, P. de Bois, S. Guillou, Numerical modeling of the effect of tidal stream turbines on the hydrodynamics and the sediment transport - application to the alderney race (raz blanchard), France, *Renew. Energy* 75 (2015) 356–365.
- [17] Shivanesh Rao, H. Xue, M. Bao, S. Funke, Determining tidal turbine farm efficiency in the Western Passage using the disc actuator theory, *Ocean. Dyn.* 66 (2016) 41–57.
- [18] <http://www.pstidalenergy.org/>. (Accessed 20 June 2016).
- [19] <http://www.snapud.com/PowerSupply/tidal.ashx?p=1155>. (Accessed 18 August 2016).
- [20] [http://www.seattle.gov/light/IRP/docs/SCLRP2008\\_Appendix\\_C.pdf](http://www.seattle.gov/light/IRP/docs/SCLRP2008_Appendix_C.pdf). (Accessed 20 June 2016).
- [21] B. Polagye, M. Kawase, P. Malte, In-stream tidal energy potential of Puget Sound, Washington, *Proc. Inst. Mech. Eng. Part A J. Power Energy* 223A (2009) 571–587.
- [22] Z. Yang, T. Wang, A. Copping, S. Geerlofs, Modeling of in-stream tidal energy development and its potential effects in Tacoma Narrows, Washington, USA, *Ocean Coast. Manag.* 99 (2014) 52–62.
- [23] Puget Sound Partnership, The 2012/2013 Action Agenda for Puget Sound, 2012, 499pp.
- [24] C. Chen, H. Liu, R.C. Beardsley, An unstructured, finite-volume, three-dimensional, primitive equation ocean model: application to coastal ocean and estuaries, *J. Atm. Ocean. Tech* 20 (2003) 159–186.
- [25] C. Chen, R. Beardsley, G. Cowles, An Unstructured Grid, Finite-volume Coastal Ocean Model: FVCOM User Manual, School for Marine Science and Technology, University of Massachusetts Dartmouth, 2006, 315 pp.
- [26] C. Chen, H. Huang, R. Beardsley, H. Liu, Q. Xu, G. Cowles, A finite volume numerical approach for coastal ocean circulation studies: comparisons with finite difference models, *J. Geophys. Res.* 112 (2007) C03018, <http://dx.doi.org/10.1029/2006JC003485>.
- [27] Z. Yang, T. Khaangaonkar, Multi-scale modeling of Puget Sound using an unstructured-grid coastal ocean model: from tide flats to estuaries and coastal waters, *Ocean. Dyn.* 60 (2010) 1621–1637.
- [28] T. Wang, T. Khaangaonkar, W. Long, G.A. Gill, Development of a kelp-type structure module in a coastal ocean model to assess the hydrodynamic impact of seawater uranium extraction technology, *J. Mar. Sci. Eng.* 2 (2014) 81–92.
- [29] Z. Yang, T. Wang, Tidal residual eddies and their effect on water exchange in Puget sound, *Ocean. Dyn.* 63 (2013) 995–1009.
- [30] D. Flater, A brief introduction to XTide, *Linux J.* 32 (1996) 51–67.
- [31] J. Smagorinsky, General circulation Experiments with the primitive equations. I. The basic experiment, *Mon. Weather Rev.* 91 (1963) 99–164.
- [32] G.L. Mellor, T. Yamada, Development of a turbulence closure model for geophysical fluid problems, *Rev. Geophys.* 20 (1982) 851–875.
- [33] P.F. Wang, R.K. Johnston, H. Halkola, R.E. Richter, B. Davidson, A Modeling Study of Combined Sewer Overflows in the Port Washington Narrows and Fecal Coliform Transport in Sinclair and Dyes Inlets, Washington, 2004, 26pp.
- [34] E. Fernandez-Rodriguez, T.J. Stallard, P.K. Stansby, Experimental study of extreme thrust on a tidal stream rotor due to turbulent flow and with opposing waves, *J. Fluids Struct.* 51 (2014) 354–361.
- [35] C. Frost, C.E. Morris, A. Mason-Jones, D.M. O'Doherty, T. O'Doherty, The effect of tidal flow directionality on tidal turbine performance characteristics, *Renew. Energy* 78 (2015) 609–620.
- [36] T. Wang, Z. Yang, Understanding the flushing capability of Bellingham bay and its implication on bottom water hypoxia, *Estuar. Coast. Shelf Sci.* 165 (2015) 279–290.
- [37] H. Takeoka, Fundamental concepts of exchange and transport time scales in a coastal sea, *Cont. Shelf Res.* 3 (1984) 311–326.
- [38] T. Wang, Z. Yang, A.E. Copping, A modeling study of the potential water quality impacts from in-stream tidal energy extraction, *Estuaries Coasts* 38 (supplement) (2015) 173–186.
- [39] N.E. Monsen, J.E. Cloern, L.V. Lucas, S.G. Monismith, A comment on the use of flushing time, residence time, and age as transport time scales, *Limnol. Oceanogr.* 47 (2002) 1545–1553.
- [40] R.A. Martin, E.A. Nesbitt, Foraminiferal evidence of sediment toxicity in anthropogenically influenced embayments of Puget Sound, Washington, U.S.A, *Mar. Micropaleontol.* 121 (2015) 97–106.